Cell cracks: power losses of up to 25% - invisible in flasher test

Summary of: Claudia Buerhop et Al.: Analysis of digitized PV-module/system data for failure diagnosis; HI ERN Helmholtz Institut Erlangen Nürnberg; 2019.

Cell cracks can cause power losses of up to 25%. But this shows only under certain conditions – room temperature like in labs is none of them. Using a flash test to detect those cell cracks therefore is not expedient. But what is able to detect this module failure?

Test site setup:
The test site contained 33 modules in 3 strings and was installed for an insurance company for validating a case. All modules (voltage and temperature measurement) and all strings (voltage and current) were continuously monitored with SunSniffer technology. In addition occacionally IR-, EL-inspections and IV-measurements have been carried out.

Results:
Tests revealed that several modules, out of them 2 especially, have cracked cells. Their power output was temporarily reduced up to 25%, depending on diverse factors, like operating conditions, temperature, etc. Mainly, the losses were seen under warm conditions and disappeared when the modules were taken from the field and reached laboratory temperature levels. **So these defects were invisible in flash tests**. Voltage of those modules was lowered significantly throughout. Therefore, SunSniffer technology was able to detect this because it measured the modules and strings in operation.

Conclusions:
Error occurancy is dynamic, spot detection systems like flashing and IR/EL will only work when module is in operation. Because of the dynamic of power loss, time series of measurement are needed to see the full coverage of power loss, and only module level monitoring with high precision sensors will be the right technology.

1. Static tests like IV measurements in the lab or snapshots like IR-/EL-imaging cannot reproduce the higly dynamic power production of cracked cells, depending on volatile operation conditions.
2. Neither are string measurements during operation able to pin down the issues.

➔ **Constant module monitoring during operation is the key** to
a) detect power reducing issues,
b) localize these, and
c) have instant actionable information without need of inspecting the plant.

SunSniffer GmbH & Co. KG
Ludwig-Feuerbach-Str. 69
90489 Nürnberg | Germany
+49 911 993 992 0
info@sunsniffer.de
www.sunsniffer.de

How can SunSniffer be applied?

For **Greenfield**: Choose modules with SunSniffer sensor inside, or choose your module manufacturer and let him take junction boxes with SunSniffer sensor inside.

For **Brownfield**: Take the Retrofit box and upgrade each module or only parts of the plant, like every 2nd string, or 30% of all modules, or…

Just contact the sales team of SunSniffer: **sales@sunsniffer.de**.

SunSniffer GmbH & Co. KG
Ludwig-Feuerbach-Str. 69
90489 Nürnberg | Germany

+49 911 993 992 0
info@sunsniffer.de
www.sunsniffer.de

Analysis of digitized PV-module/system data for failure diagnosis

Claudia Buerhop[1], Tobias Pickel[1], Janine Teubner[1], Bernd Doll[2,3], Jens Hauch[1], Christoph J. Brabec[1,2]
[1]HI ERN Helmholtz Institut Erlangen Nürnberg, D-91058 Erlangen, Immerwahrstraße 2
[2]i-MEET, FAU Erlangen Nürnberg, D-91058 Erlangen, Martensstraße 7
[3]Graduate School for Advanced Optical Technologies, D-91052 Erlangen, Paul-Gordan-Str. 6

c.buerhop-lutz@fz-juelich.de, Tel.: 0049-9131-9398-177, FAX: 0049-9131-9398-199

ABSTRACT EL-images disclose many failures in PV-modules, e. g. cell cracks. Their impact and the relevance of certain defect features on the performance during operation is not known. This study focused on the identification of defective power-relevant cells, their impact on the performance and the degradation. Therefore, pre-cracked, low-performing modules are integrated in a string and monitored on module level. As a result, a statistical analysis of EL-images identified the power-relevant cells. The power of defective modules is extremely sensitive to changing measurement conditions. Historical monitoring data and actual EL-images give evidence that so far no changes of the crack structures of fractured cells occurred. Strong seasonal impact is observed. However, the yield is rather stable during the inspection period.
Keywords: system performance, cell cracks, IR-imaging, EL-imaging, monitoring

1 INTRODUCTION

The demand for quality control of PV-systems has increased during the last years. Many methods have been developed and are used. Thermography (IR-imaging) with and without drones, electroluminescence (EL) imaging, IV-curve measurements and monitoring belong to the most used technologies. All of these methods provide helpful data for detecting, identifying, localizing, or quantifying defective components or modules in a PV-system. However, none of these techniques are able to deliver all the data of interest alone. For example, IR- and EL-imaging are a snapshot and can visualize and locate a defect, but do not give the influence on the electric yield of the compromised modules and strings. Monitoring data consist of many electrical parameters measured continuously with a high temporal resolution during the lifetime of a PV-system. Signal noise and uncertainty limit the detection of defects. Localizing weak-performing modules is not possible with string level monitoring.

With this paper, we address the relevance of detected irregularities in IR- and EL-images for the module and string performance, respectively the power output. Therefore, data from the lab are compared to field data, see Figure 1. Furthermore, the recognition of performance-relevant defects as well as their degradation will be discussed. This paper concentrates on the analysis of the performance of PV-modules with cracked cells:

1. Identification of power-relevant cracked cells
2. Impact on performance, e.g. voltage, power, yield, performance ratio
3. Degradation of modules with cracked cells

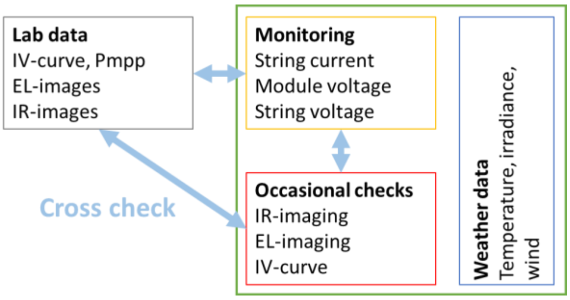

Figure 1: Scheme showing all data recorded at the test facility necessary for a cross check

2 EXPERIMENTAL PROCEDURE

We investigated a well characterized PV-system with 33 pre-cracked PV-modules installed in Northern Bavaria at a test facility. The modules were connected in three strings. Monitoring took place on the module level as well as on the string level with sensors from SunSniffer. In addition since June 2019, the best performing module was operated independently of the remaining string as a reference module by utilizing a module optimizer. The voltage and junction box temperature were recorded for each module and the current and voltage of each string. Parallel to the module data, a weather station at the test facility recorded meteorological data, e. g. ambient temperature, solar irradiance, and wind speed as well as wind direction. The time resolution is less than one minute.

Besides the continuous data collection, IR- and EL-inspections as well as IV-measurements were carried out occasionally throughout the years. Data on the module-level exists for more than one year. On April 19th, 2018 a well-performing module was replaced by the poor-performing module A (relative power of 92%).

Furthermore, all modules were analyzed in the lab before the installation in the field. IV-curves were measured under standard test conditions with a solar simulator. The module power ranged from 198 W to 230 W with 86% to 100% of the nominal power, respectively. EL-images and IR-images were recorded, too.

3 RESULTS AND DISCUSSION

3.1 Identification of power-relevant cracked cells

IR-imaging is a sensitive technique used to visualize bad-performing cells, especially under operating conditions. Since in defective cells the absorbed sunlight produces less electrical power than in healthy cells, the temperature in such cells is increased [1]. Depending on the failure mechanisms, the electrical power loss and consequently the temperature rise in these cells can be very high, up to several K.

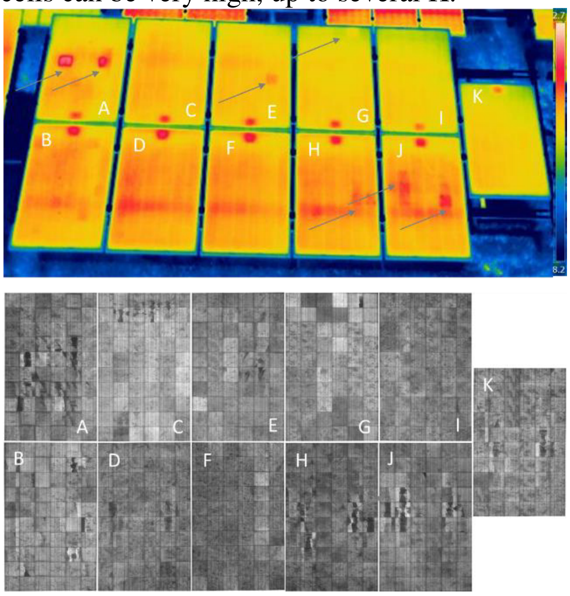

Figure 2: Visualization of the modules at the test facility, top: IR-overview of the modules of one string showing certain modules with IR-irregularities (indicated with an arrow), bottom: El-images in same order, letters A – K identify the modules, July 3rd, 2018

Figure 2 shows IR-images and EL-images of all 11 modules of a string. This powerful combination of imaging methods is used to study and identify the power-relevant cracked cells. Under operating conditions, the IR-image shows that several modules (A, E, G, H, J) display irregularities. The EL-images illustrates many modules with obviously cracked cells (A, B, C, D, E, G, H, J, K). Dark areas indicate electrically isolated areas, called cell fragments. Some correlate with cells with elevated temperature $1 < \Delta T < 10$ K, others not, although their appearance in the EL-image is similar. Highest cell temperatures are reached in module A, $\Delta T_{\text{left cell}} \approx 10$ K and $\Delta T_{\text{right cell}} \approx 5$ K.

A developed statistical analysis of the EL-images (described in [2]) reveals the relevant differences between cracked cells, which are hard to catch by the naked-eye. Therefore, the cell area of a pre-defined EL-intensity, which is related to the electrical contact of the cell fragments, is determined. The specific EL-intensity was set to 20% of the median of the EL-intensity by experience. Figure 3 presents and marks the critical and potentially power-relevant cells in the modules. In modules A, G and J, cell fragments are larger than 10% of the cell area, which is above the critical threshold for this module type related to [3]. In modules B, E and H, the area is less than 7%. In good agreement with Figure 1, the marked red cells correspond to irregularly heated cells detected by IR-imaging. Thus, critical, power-relevant cracked cells can be distinguished from uncritical cells using this statistical approach. However, discrepancies are possible because of the sensitivity of crack structures to various factors, e. g. module temperature, string configuration, and operating conditions

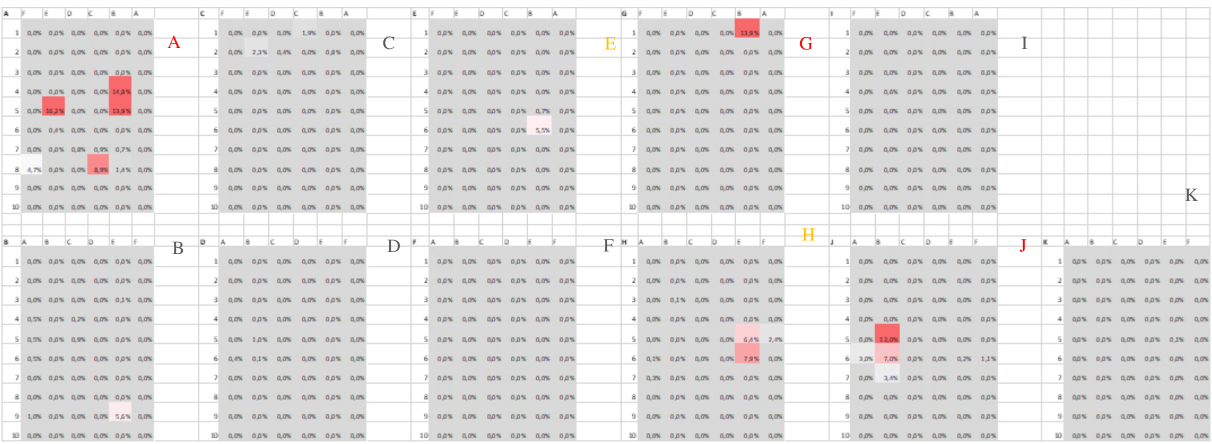

Figure 3: Statistical EL-image evaluation presenting the most critical cells and their fragment size, in identical order as in Figure 2. With increasing intensity of red the negative impact of the cell on the module performance increases

3.2 Performance, power of defective modules

Typically, the performance of a module is described by its IV-curve and its power at maximum power point (mpp). Various measurements are available to measure the power of a PV-module. Table I lists three differing setups: I) Measurement of the IV-curve under standard test conditions (1000 W/m², 25°C) in the lab, II) Measurement of the IV-curve in the field at varying irradiance and module temperature, and III) evaluating module monitoring data (current, voltage) under the module's real operating conditions. Using method III mimics the real situation best since interactions of the modules in the series connection, e. g. shifts of the operating point, are taken into account [4].

Table I: List of power measurements including conditions for the field measurements (see Figure 6)

	Configuration	*site*	*Irradiance W/m²*	*Module temp. in °C*
I	1 module	Lab	1000	25
II	1 module	Field	950 ± 50	43
III	1 module in a string	Field	970 ± 70	59-63

The IV-curves in Figure 4 visualize that module A and J have a reasonably reduced power output and I_{mpp} and V_{mpp} differ from the ones of the other modules. This holds true also for individual power measurement of the modules in the field. However, to know the performance under operating conditions, the electrical serial connection in a string has to be considered. Figure 4 visualizes the shift of the operating voltage under string conditions for defective modules. Consequently, the voltage of A and J are considerable lowered at the operating point within a string.

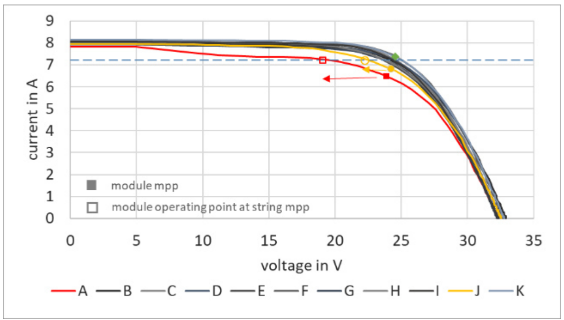

Figure 4: Visualization of the shift of the operating point of defective modules A and J within the string, at irradiance E = 1000 W/m²

Similar observations can be made for the power generation throughout a day, exemplarily shown for a sunny day in Figure 5. For better comparison, the ratio between the module power and the string power is plotted. If all modules contribute equally to the string power, the ratio would be expected to be 9.1%. It is clearly visible that module A and J perform worse than the other modules during the day. The increasing scatter of the data, especially for module A, is a strong indicator for the presence of a defective module, because during mpp-tracking the defective module's voltage changes over a wider voltage range than the one of good modules, see Figure 4 [4, 5].

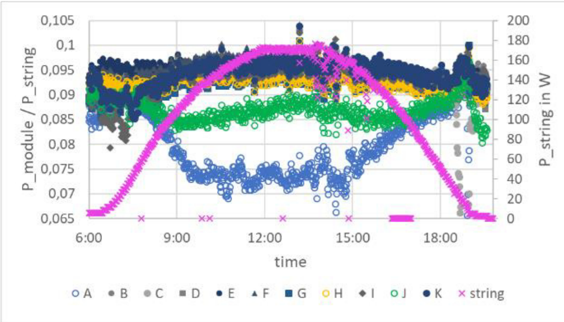

Figure 5: Relative module power, June30th, 2019

The comparison of the power data of method I, II, and III are shown in Figure 6. It is obvious that module A performs worse than modules J and H, which in turn perform worse than the others. However, the power levels differ among the modules, which is caused by the increased module temperature for the field measurements and additionally by the shift of the individual operating point to a string operating point for the monitoring data.

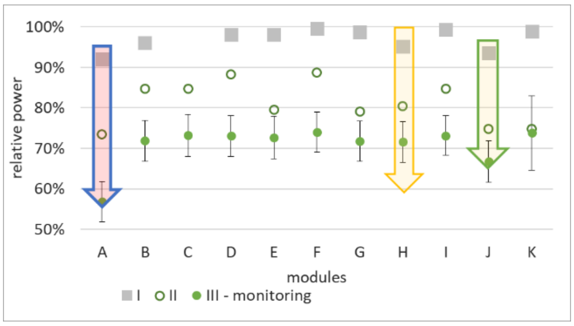

Figure 6: Relative module power measured in the lab, in the field (May 23rd, 2019), on the basis of the monitoring data on June 28th, 2019, and on basis of an ideal string for June 30th, 2019

Furthermore, temperature differences and varying measurement conditions influence the module performance and the measurement so that fluctuation of the data occurs, as seen for the data of method II. Figure 7 depicts the interacting TOP-factors: module temperature distribution T, operating conditions O, and electrical power output P. These involve various parameters, e. g. for T: heat transfer, weather conditions and irradiance, for O: operating point (voltage, current) module temperature, inverter specification, and curtailment, and for P: module and cell technology, and failure type. It is a sensitively balanced system - if one parameter changes, the others are affected too. For example, if the electrical contact of a cracked cell is closed, the cell temperature decreases, the power output increases, and the operating point shifts.

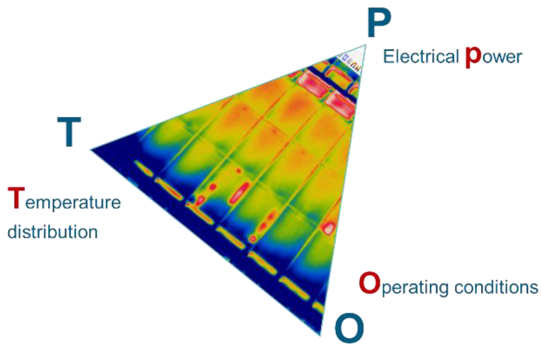

Figure 7: Module and PV-system performance determining and interacting TOP-factors: temperature T, operating conditions O and electrical power P

3.3 Degradation study of defective modules

Degradation is a persistent and long-lasting destruction or a loss of material properties. For PV-modules the important properties are power output, yield and performance. In order to detect degradation, data at several dates have to be collected and compared. EL-images are predestinated to disclose and localize changes in cell structures. For continuous, creeping changes as well as spontaneous modifications, especially affecting the electrical parameters, monitoring data are advantageous.

Module and string data are recorded for almost two years up to now. Figure 8 illustrates the mean daily module V_{mean} and string voltage $V\_{mean,string}$, the daily accumulated module V_{sum} and string voltage $V\_{sum,string}$, and the performance ratio of the modules PR_{module} and the string PR_{string}. The mean string voltage is rather constant throughout the year; all modules suffer from a significant voltage drop of at least 4 V during the hot summer period. The accumulated voltage follows the irradiation. In sun-rich summer months, the voltage is high and drops strongly during the winter months. The performance ratio is about 62 – 78% for modules and the string during the summer months. Modules A and J attract attention due to their low values in all graphs, voltage data as well as the performance ratio. However, a degradation or negative evolution with time is not recognizable. Such effects may be hidden by weather-related influences.

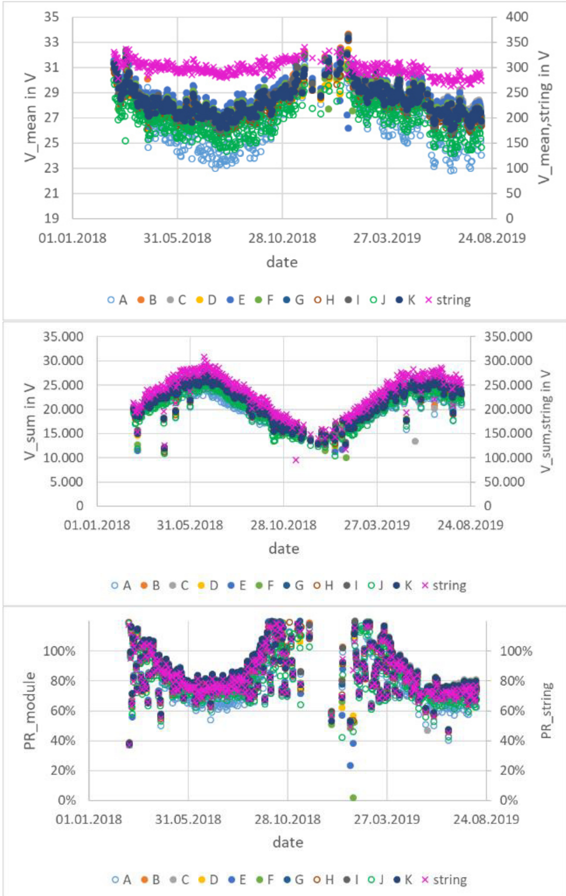

Figure 8: Mean voltage V_mean (top), accumulated daily voltage V_sum (middle), performance ratio PR of the modules and the string (bottom)

To overcome seasonal effects, a ratio between the module data and the string data are calculated. Figure 9 shows the ratios of V_{sum}, PR, and yield Y. During the winter months only few data exist because of filtering with respect to irradiance and current. If all modules perform identically, the ratio would be 9.1%. Deviations indicate differing performance. During the sun-rich months from March to October almost constant ratios close to $V\_{sum} = 9.2\% \pm 0.7\%$ are realized for most modules. The voltage over the course of the year differs for modules A and J. It is evidently lower. While module J exhibits the same small voltage scattering as the good modules, module A stands out by its large variation of voltage. Reasons for the extended scattering of the data are presumably the rather flat IV-curve, which results in large voltage changes for small current shifts, and the observed volatile crack structure due to temperature changes.

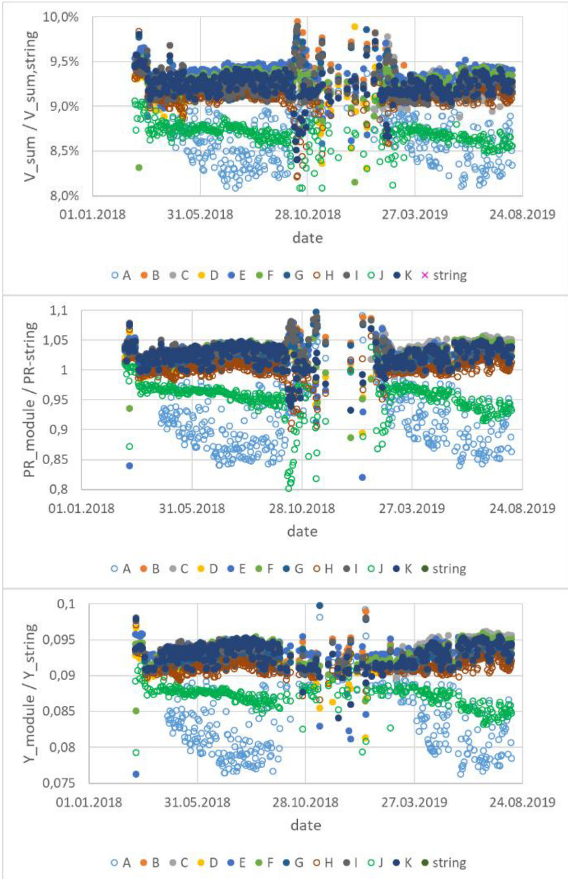

Figure 9: Ratios of accumulated voltage V_sum (top), performance ratio PR (middle) and yield Y (bottom) of the modules

Furthermore, the plots depict clearly that the difference between the ratios of A and J and the well performing modules increase throughout the year. There is a negative linear trend, which seems to end at the end of the year. The data show an annual periodicity because of the same linear seasonal summer performance in the following year. As a first approach, the trend is described by a simple linear regression

$$\frac{dR}{dt} = 9\% - m \cdot (t + T) \,,$$

with R a ratio (e.g. $V_{\_sum,module}$ / $V_{\_sum,string}$), 9% is the starting value, *m* the slope (ratio change with respect to one year), *t* time in days, and *T* the annual periodicity. Calculated values for *m* are given in Table II. The *m*-values for $V_{\_sum}$ and *Y* are very similar, which indicates a dominating impact of the voltage on the yield.

Table II: Performance loss values for various ratios

R	*Module A m in %/a*	*Module J m in %/a*
V_sum	2.1	2.1
PR	8.6	5.2
Y	2.1	2.0

For a better understanding of the long-term evolution, the yield is accumulated and its ratio calculated, see Figure 10. While the well performing modules have ratios in the range of 9.2% to 9.4%, now three modules show outstanding lower ratios and poorer performance. Module H shows a ratio of 9.1%, module J in the range of 8.8 to 8.7% and module A from 8.4% to 8.2%. both with decaying tendency. During the winter months the values are fairly constant. While in spring they start to decrease again slowly. Besides the strong performance loss of module A after its installation on April 19th, 2018 and a subsequent adaption phase to the ambient and operating conditions, no exceptional or increased performance drop is observed so far. The defective modules do not degrade faster or stronger than the others.

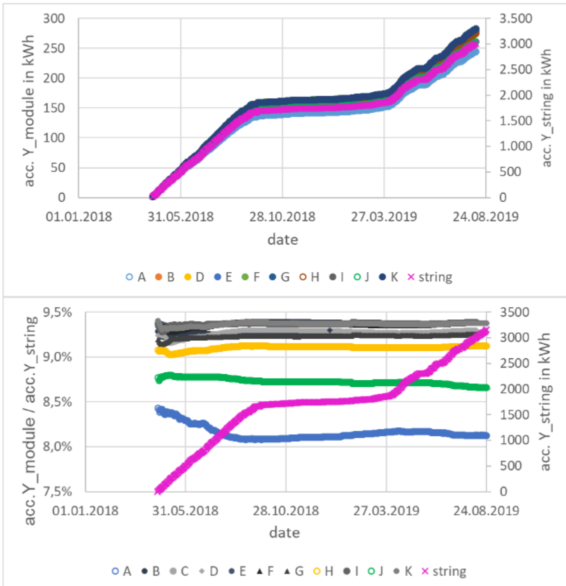

Figure 10: Accumulated module and string yield (top) and accumulated yield ratio (bottom)

What is interesting is the loss of yield due to the existing defective modules. Therefore, the string yield is compared to an ideal string operated under the same conditions. The ideal, defect-free module string is calculated on the basis of the data from a reference module. Figure 11 shows the measured string data and the calculated ideal string yield. The yield loss due to the presence of defective modules is between 0.6 and 1.4 kWh per day. In summary, 7% of the potential yield is lost.

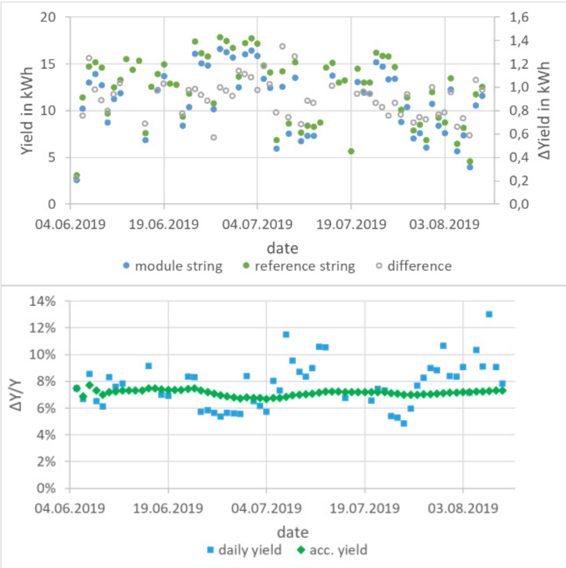

Figure 11: Measured string yield and fictive string yield based on data from an optimal operating module

Finally, the existing weather conditions during the degradation study are of importance to pigeonhole the relevance of the outcome. The test facility is located in a rural Bavarian region in Central Europe in a moderate, continental climate region. Figure 12 illustrates the wind gusts and the ambient temperature at the installation site during the observation period. At least, two strong storm events were present with maximum wind speeds of about 18.1 m/s on January 18th, 2018 and with 18.9 m/s on March 9th, 2019.

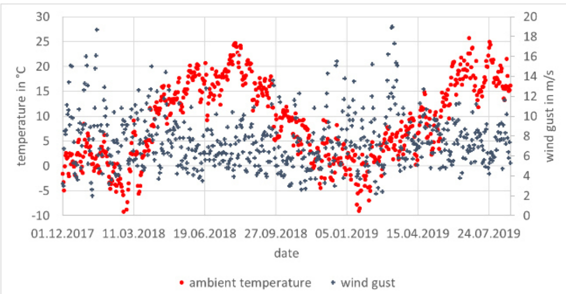

Figure 12: Weather conditions, mean ambient temperature, maximum daily wind speed, throughout the inspection period 1. Dec. 2017 – 26. Aug. 2019

In summary, no increased degradation in terms of power loss and no change of crack structures in the EL-image of the pre-cracked PV- modules due to normal operating conditions were observed. The modules perform, as expected, worse than intact modules and decrease the outcome of the string. So far, the defective modules do not cause excessive degradation.

4 CONCLUSION

IR- and EL-image snapshots and continuous monitoring data are complementary methods to detect, explain and understand the performance and degradation of module failures. Suitable heuristics need to be developed for effective data analysis. Performance-relevant cracked cells can be recognized by statistical analysis of EL-images. Using module monitoring, different performance mechanisms that are undetected by string data analysis can be tracked. So far, the defective, pre-cracked PV-modules do not cause excessive degradation. Further work will provide more insight for an effective mix of methods yielding a smart PV-inspection in the future.

5 ACKNOWLEDGEMENT

HI ERN gratefully thanks the German Federal Ministry for Economic Affairs and Energy (BMWi) for financial funding of the project COSIMA.

The authors sincerely thank the Allianz Risk Consulting GmbH / Allianz Zentrum für Technik (AZT) in Munich, Germany for supporting the project with a large number of PV-modules. Furthermore, we thank SunSniffer GmbH & Co. KG in Nürnberg for providing the necessary sensors for monitoring the PV-system on module level.

6 REFERENCES

[1] J. A. Tsanakas, et al.; Renewable & Sustainable Energy Reviews 62 (2016) 695 Tsanakas, John A. Ha, Long Buerhop, Claudia.
[2] C. Buerhop-Lutz, et al., 36th EU-PVSEC (2019).
[3] M. Köntges, et al.; Sol. Energy. Mater. Sol. Cells 95 (2011) 1131.
[4] C. Buerhop, et al., 29th EU PVSEC (2014) 3260.
[5] R. Moretón, et al.; Solar energy 118 (2015) 28.